MATERIAL CHARACTERIZATION OF ADDITIVELY MANUFACTURED PA12 AND DESIGN OF MULTIFUNCTIONAL SATELLITE STRUCTURES

Simon Hümbert [(1)], Lukas Gleixner [(1)], Emanuel Arce [(1)], Patrick Springer [(2)], Michael Lengowski [(3)], Isil Sakraker Özmen [(1)]

[(1)] Deutsches Zentrum Für Luft- Und Raumfahrt e.V., Pfaffenwaldring 38-40, 70569 Stuttgart, Germany, Email: simon.huembert@dlr.de, l.gleixner@gmail.com, emanuel.arce@dlr.de, isil.sakraker@dlr.de
[(2)] Fraunhofer-Institut für Produktionstechnik und Automatisierung IPA, Nobelstr. 12, 70569 Stuttgart, Germany, Email: patrick.springer@ipa.fraunhofer.de
[(3)] Universität Stuttgart Institut für Raumfahrtsysteme (IRS), Pfaffenwaldring 29, 70569 Stuttgart, Germany, Email: lengowski@irs.uni-stuttgart.de

ABSTRACT

Increasing cost pressure on satellite builders and their suppliers push the motivation to open up for new designs and processes. This paper investigates the applicability of thermoplastic additive manufacturing for mass production of satellites. First, the potential of the cost-effective 3D-printing material Polyamide 12 for space structures is examined. Tests include mechanical and thermal-vacuum properties. In the second step, a multifunctional technology demonstrator is designed and a first qualification test is performed. This demonstrator integrates electronic and thermal management components and shows considerable volume savings. Additionally, the automatable processes used for manufacturing enable further cost reductions in series production.

1 INTRODUCTION

Faster and cost efficient access to space necessitates the inclusion of innovative technologies in space applications in contrast to the conventional techniques which are flight qualified but come with very high costs and very long development/qualification time scales.

Especially, satellite constellations where a serial production of satellites is required, automated, flexible and highly reliable processes for low costs are indispensable. It is the aim of the IRAS (Integrated Research Platform for Affordable Satellites) consortium to investigate architectures and technologies for future low cost space missions. It currently focuses on satellite constellations of about 100 satellites at LEO obits. One of the main tasks of IRAS is to investigate suitability of the materials, techniques such as additive manufacturing and electronics technologies from the automotive industry, which is very capable of mass production and high reliability simultaneously. These technologies combined, will allow for more flexible solutions and eventually will lead to new in-orbit capabilities in the near future.

Today, most thermoplastic 3D-printed satellite structures are developed within academic projects at a low budget. Examples are the UNSW ECO [1] or the Tomsk-TPU-120 [2], where the entire satellite bus is manufactured additively. Other projects like the RAMPART 2U CubeSat [3], KYSAT-2 [4], PRINTSAT [4] or SnapSat [5] include integrations of electronics and sensors into the structure by additive manufacturing.

These examples already show that integrating electronics is a major issue regarding 3D-printed, thermoplastic satellite structures, especially in conjunction with CubeSats. There are several ways to include conductive paths into the structure. References [6–8] present a new technology, Fiber Encapsulation Additive Manufacturing (FEAM), which is capable of embedding wires directly during the printing process. Related processes are presented by [9] and [10], where the wires are heated and embedded in a thermoplastic substrate. Another possibility are conductive inks, applied by Direct-Write processes [10]. It is also possible to print conductive filaments [11] and low melting metals [12] with a Fused Filament Fabrication (FFF) printer, or conductive particles with a SLS-printer [13]. The last possibility of integrating conductive paths to be mentioned is manually including pre-assembled cables during the printing process. This way, printed cavities can include entire harnesses [14,15].

Further 3D printed multifunctionality is the integration of batteries. Printed battery housings are already flying in the CubeSat KySat-2 [16] and by NASA [17].

Similar integration concepts have been shown for sensors. SnapSat [5] contains an embedded magnetic field sensor, [18] demonstrated embedded acceleration sensors and [19,20] and [21] GPS, temperature and contact sensors, respectively.

Using the integration processes mentioned so far, it is possible to integrate several other electronic components, e.g. antennas [9,15] and small circuits [10,22] have successfully been embedded into thermoplastic substrates.

In addition to electrical component integration, there is progress in propulsion components. A small electric thruster has completely been embedded into the structure by [23]. Furthermore, attempts of integrating cold gas systems have been done by [24].

Finally, additives can be used to locally generate

specific material properties for thermal management (thermal conductivity) [25] or for electromagnetic interference (EMI) shielding [26].

The aim of this paper is to demonstrate the potential of a low-cost, multifunctional satellite structure by automatable, additive processes. In the first step, the usability of the standard 3D-printing engineering material Polyamide 12 (PA 12) for satellite structures is tested. This material is easy to process and its wide range of applications provides a lot of experience in mass production (e.g. in automotive industry). Additionally, short carbon fiber reinforced PA for FFF printing is available. This reinforcement improves the mechanical and thermal properties and is promising to enable the application of PA in structural space applications. Therefore mechanical and thermal-vacuum properties of the carbon fiber reinforced FFF material and pure PA processed by a SLS (selective laser sintering) printer are tested for reference. The SLS printed PA has very homogeneous properties and is comparable to industrial processes like injection molding.

In the second step, a multifunctional demonstrator is designed. The structure is a sandwich with a 3D-printed honeycomb core. On the one hand, this makes so far unusable design space available. On the other hand, it can be manufactured by highly automatable and flexible processes, for example by a combination of FFF printing and automated fiber placement (AFP). The demonstrator structure is used to show the possible solutions for integrating functions into the structure by 3D-printing. Furthermore, it demonstrates the potential of multifunctional structures for future satellites. To demonstrate the applied integration concepts, an additional shaker specimen is designed and tested.

2 MATERIAL CHARACTERIZATION

2.1 Materials

The tested carbon fiber reinforced polymer is Nylon 12CF from Stratasys [27]. It is a polyamide 12 (PA 12) resin and contains chopped carbon fibers, at a load of 35 % by weight. The SLS PA is a polyamide 12 based resin, trading name PA 2200 Balance 1.0, from EOS [28].

2.2 Material Testing

The testing of the two PA materials includes mechanical, thermal vacuum and outgassing tests. Mechanical tensile tests are performed according to the standard ASTM D638-10. Measured results are the tensile ultimate strength as well as the Young's Modulus. Specimens were produced in three different orientations as shown in Fig. 1. For the in plane orientation, two sets of specimens were produced. One of those sets was exposed to thermal vacuum cycling. Using these specimens, the test results, before and after thermal vacuum cycles, were compared to identify possible changes in material properties.

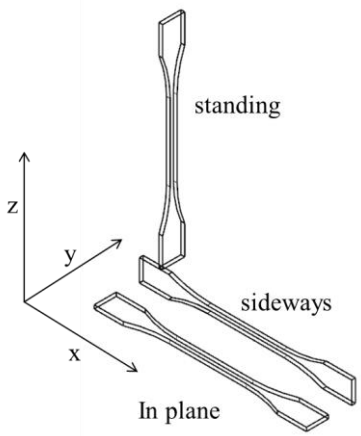

Figure 1. Tensile specimen orientation

Thermal vacuum cycling consists of 100 cycles. 25 cycles have a temperature range of -40 °C to 80 °C and 75 cycles have a range of -30 °C to 80 °C. The vacuum during cycling is 10^{-4} mbar. Temperature during the cycling is measured by to sensors attached to two individual specimens.

2.3 Test Results

The mechanical test results of FFF printed reinforced PA (PA12-CF) and the SLS printed pure PA (PA12-SLS) before thermal vacuum cycling are summarized in Fig. 2 and Fig. 3..

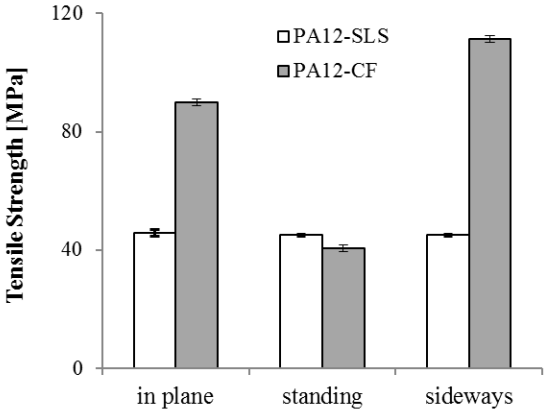

Figure 2. Tensile strength of SLS processed PA 12 (PA12-SLS) and short carbon fiber reinforced FFF processed PA 12 (PA12-CF)

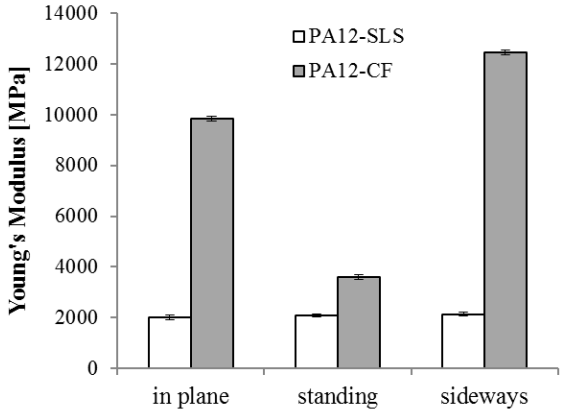

Figure 3. Young's modulus of SLS processed PA 12 (PA12-SLS) and short carbon fiber reinforced FFF processed PA 12 (PA12-CF)

The SLS processed pure PA shows mechanical properties very similar to the manufacturer specifications. It also does not show significant anisotropy with respect to the printing orientation. The carbon fiber reinforced PA, on the other hand, shows a strong anisotropy. Regarding the in plane and sideways specimens, tensile strength is drastically increased by the reinforcement. The standing specimens, on the other hand, show reduced strength. Similar behavior can be observed regarding the Young's Modulus. Young's Modulus of the reinforced material, however, is always above the pure PA. Furthermore, it can be noted, that the standard deviation off all tests is less than 5 %.

The effect of thermal vacuum cycling on the mechanical properties is shown in Fig. 4 and Fig. 5. In both cases, thermal vacuum cycling leads to a slight improvement of mechanical properties. At the same time, elongation at break is reduced.

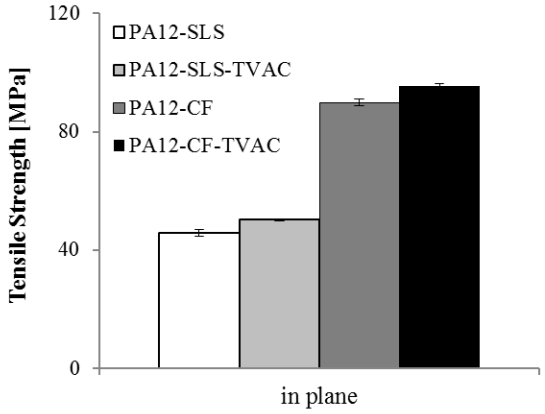

Figure 4. Tensile strength of PA 12 and short carbon fiber reinforced PA 12 before and after (-TVAC) thermal vacuum cycling

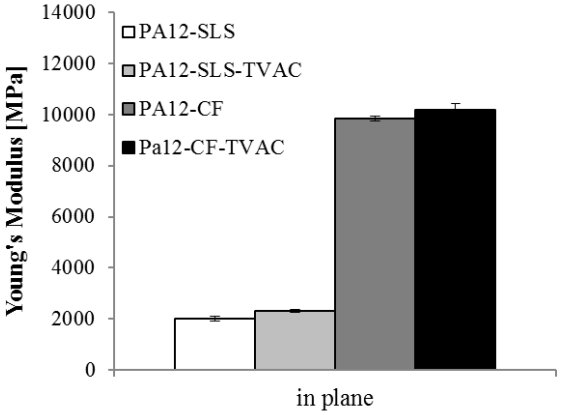

Figure 5. Young's Modulus of PA 12 and short carbon fiber reinforced PA 12 before and after (-TVAC) thermal vacuum cycling

2.4 Material selection

The tested PA, especially the fiber reinforced PA, shows potential for low-cost space application. However, a qualification process will require an elaborate test program. Alternatively, ECSS-Q-70-71a recommends two other thermoplastics, that are available for 3-D printing, PEI (Polyetherimide) [29] and PEEK (Polyether ether ketone) [30]. Both materials are high temperature engineering thermoplastics with very good mechanical properties.

Tab. 1 shows the range of potential materials and their properties. The PA 12 mechanical properties represent the test results shown before. The FFF printed carbon fiber reinforced PA yields the highest strength and stiffness of the shown materials and is due to its easy printability a considerable material for multifunctional structures. Additionally, it is significantly cheaper than PEI or PEEK. However, the low glass transition temperature of PA does not allow the full operating temperature range of low earth orbit missions. Therefore, this material can only be used in controlled temperature environments (e.g. internal payload modules). For outer surfaces, the well printable PEI can be used or for very high loaded parts, the strong and also more expensive thermoplastic PEEK can be used.

Table 1 Property range of potential FFF materials

Material	Young's Modulus [MPa]	Tensile Strength [MPa]	HDT*/Tg** [°C]	CTE [10^{-5}/K]
PA 12 [28]	ca. 2000	ca. 45	NA/40	10.9
PA 12 CF [27]	3800 - 12000	40 - 112	143/NA	NA
PEI [29]	2150 - 2270	42 - 69	153/186	6.5
PEEK [30]	4250	90	165/164	4.7

*HDT = Heat deflection temperature / **Tg = Glass transition temperature

3 DEMONSTRATOR DESIGN

A technology demonstrator is developed to verify feasibility and functionality of the function-integration for additively manufactured satellites. The potential functions for integration in a satellite structure by 3D-printing explained in Section 1 can be summarized in 3 topics:

- Electronic components
- Propulsion components
- Thermal management components

The most promising function-integrations that can be realized with the resources of the IRAS project partners were implemented in this demonstrator. The functions include electronic as well as thermal management components. An integration of propulsion components is not feasible within the given project.

To enable a direct comparison and a realistic assessment, the support structure of the GPS receiver box of the "Flying Laptop" satellite [31] is realized in the integrated design. The wire harness of the GPS-box consists of three different cable types: AWG 26 data lines, AWG 24 power lines and coaxial cables. While the power lines can be integrated directly via ultrasonic embedding, the data lines need an EMI-shielding to prevent a malfunction in data processing. Thus the data lines are grouped to cable bundles which are surrounded by a copper braid sleeve. Those bundles and the coaxial cables are integrated in the 3D-printed cable ducts. In order to connect the integrated cables with other modules, micro-D connectors are integrated together with the cables. Furthermore a temperature sensor, a heating foil, joining elements and a combined gyroscope and acceleration sensor are integrated in the honeycomb core. The gyroscope and acceleration sensor is a combined MEMS sensor designed for the automotive industry. It is currently space qualified by the IRAS project partner Fraunhofer IPA. Contrary to the sensors which are integrated together with the wiring harness in cavities at the end of the printing process, the nuts for mounting the GPS box are inserted and imprinted during the printing process. An exploded view of the complete module with GPS box and cover layers is shown in Fig. 6.

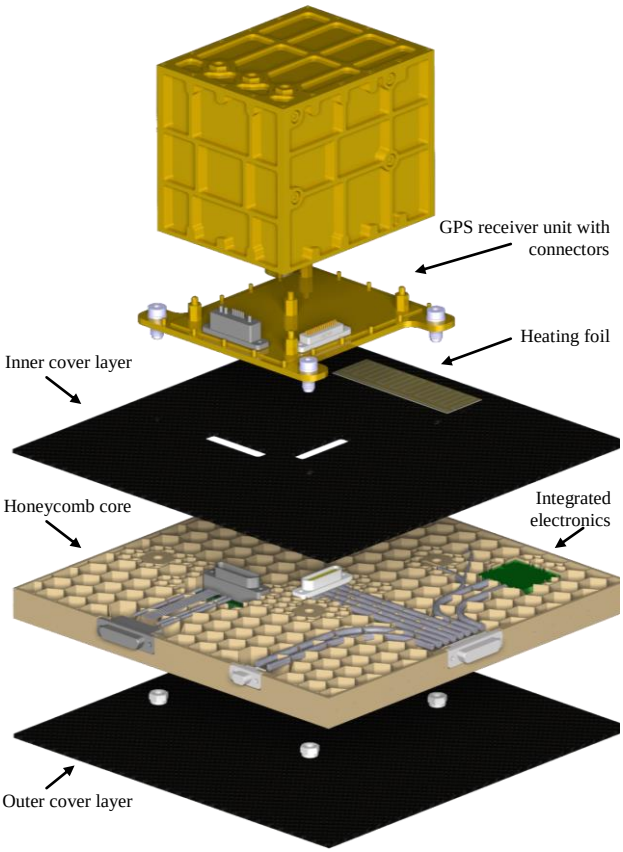

Figure 6. Exploded view of the technology-demonstrator with the GPS receiver unit

In order to provide the proof of concept for the demonstrator and to investigate the behaviour of the integrated electronics under the loads at the launch, a first test component was produced and submitted to a vibration testing. Most of the planned functions are integrated in the test component: a connector, a gyroscope sensor, shielded cable bundles, an ultrasonic embedded wire and a coaxial cable (Fig. 7 (a)).

To ensure that results on the functionality of the concept are available before the optimization of the printing process for the PEI honeycomb core, the test component is manufactured with a PETG honeycomb core. The Young's modulus of PETG is with 2040 MPa similar to that of PEI (compare Tab. 2). If the full functionality of the electronics can be verified after the test, this can also be expected for a honeycomb core made of PEI.

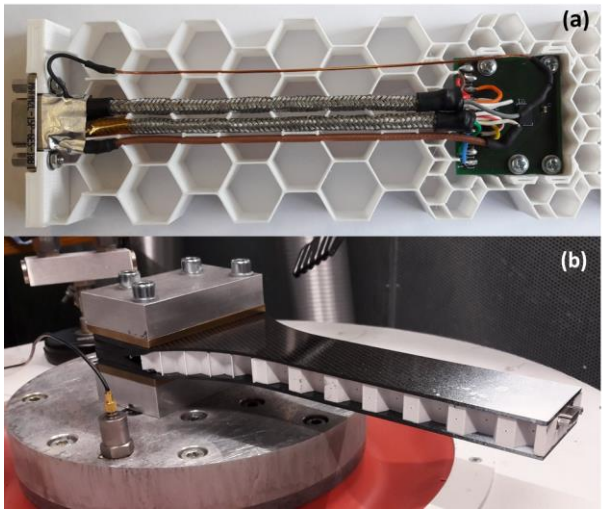

Figure 7. Test component for vibration testing;(a) the printed honeycomb core with integrated electronics; (b) the complete test component mounted on the shaker

The test component was subjected to a vibration test plan which includes a random vibration load (RVL) and a High Level Sine Sweep (HLSS). The duration of the random vibration is 120 second and the sweep rate of the sine test is 2 Oct/min. The load specifications are shown in Fig. 8 and Fig. 9. The test setup is shown in Fig. 7 (b).

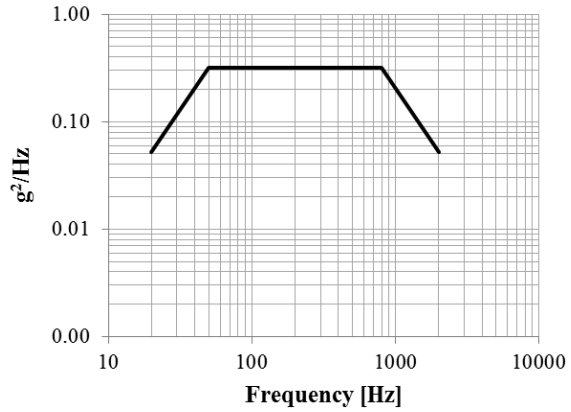

Figure 8. Random vibration load (RVL)

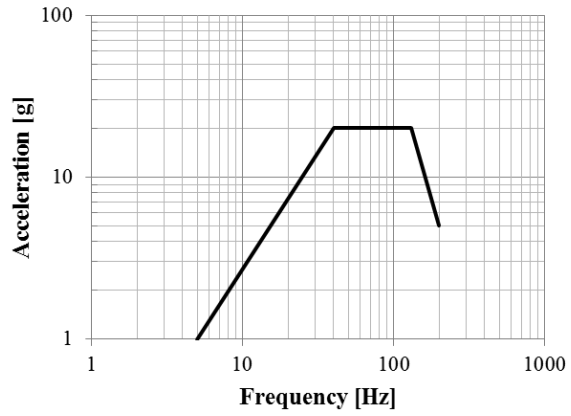

Figure 9. Sine vibration load (HLSS)

After the test, no visible damage can be detected and the complete functionality of the electronic system can be verified. Furthermore, no change in the natural frequency is detected, which would be an indicator for internal damage. The natural frequency of the test component in the range from 0 to 2000 Hz is found at 230-240 Hz (Fig. 10).

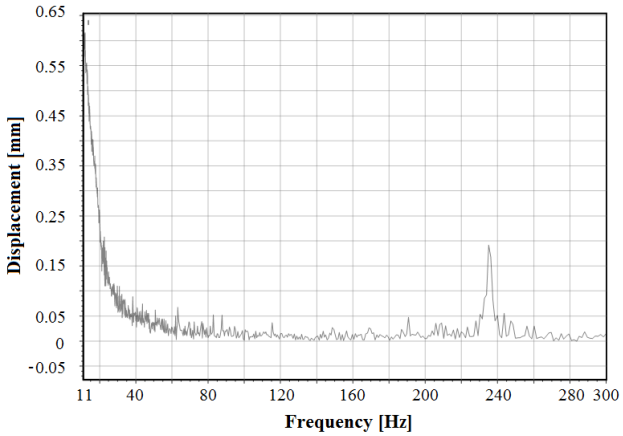

Figure 10. Modal analysis of the test component at 0,3g

4 CONCLUSION & PERSPECTIVES

The tested mechanical and thermal vacuum properties of carbon fiber reinforced PA 12 indicate its potential for future space applications. In addition, FFF materials are specially design for reduced water absorption, which is beneficial for a space qualification. However, several other tests have to be performed before the material can actually be applied to a space structure. In particular outgassing tests will be a follow on step within the project.

The technology demonstrator points out the capability of multifunctional sandwich structures for satellites. The concept makes so far unusable design space accessible and can generate considerable volume savings. A First successful vibration test confirms the design. A weight reduction, on the other hand, is unlikely since printed honeycomb is not lighter than standard aluminum honeycombs. However, the multifunctional structure offers further cost saving by an automated production suitable for mass production and reduced assembling costs.

A holistic evaluation of the presented concept requires several further steps. Especially the interaction of different coefficients of thermal expansion under thermal vacuum conditions has to be investigated. Additionally, a comprehensive cost analysis has to be performed to give detailed information on cost savings and feasible business cases.

5 ACKNOWLEDGEMENTS

This study is funded by Ministerium für Finanzen und Wirtschaft Baden-Württemberg, Germany under the contract no: 3-4332.62-DLR/49.

6 REFERENCES

[1] The Australian Centre for Space Engineering Research, "UNSW-EC0 QB50 CubeSat 3D Printed Structure (ACSER): 3D Printed Structure." [Online]. Available: http://www.acser.unsw.edu.au/3d-printed-structure.

[2] H. J. Kramer, "Tomsk-TPU-120: The first 3D printed CubeSat Mission," 2016. [Online]. Available: https://directory.eoportal.org/web/eoportal/satellite-missions/t/tomsk-tpu-120.

[3] G. Moore *et al.*, "3D Printing and MEMS Propulsion for the RAMPART 2U CUBESAT," in *24th Annual AIAA/USU Conference on Small Satellites*, 2010.

[4] W. Clements *et al.*, "3D printed parts for CubeSats: Experiences from KySat-2 and PrintSat using Windform XT 2.0," presented at the Advances in the Astronautical Sciences Second IAA DyCoss, 2014, vol. 153.

[5] C. Shemelya *et al.*, "Multi-functional 3D printed and embedded sensors for satellite qualification structures," in *IEEE SENSORS 2015*, Piscataway, NJ, 2015.

[6] B. Cox, M. Saari, B. Xia, E. Richer, P. S. Krueger, and A. L. Cohen, "Fiber Encapsulation Additive Manufacturing: Technology and Applications Update," *3D Printing and Additive Manufacturing*, vol. 4, no. 2, pp. 116–119, 2017.

[7] M. Saari, M. Galla, B. Cox, E. Richer, P. Krueger, and A. Cohen, "Active Device Fabrication Using Fiber Encapsulation Additive Manufacturing," in *Proceedings of the International Solid Freeform Fabrication Symposium 2015, Austin, Texas*, .

[8] B. Xia, M. Saari, B. Cox, E. Richer, P. S. Krueger, and A. L. Cohen, "Fiber Encapsulation Additive Manufacturing: Materials for Electrical Junction Fabrication," in *Proceedings of the 27th Annual International Solid Freeform Fabrication Symposium 2016 - an Additive Manufacturing Conference*.

[9] E. Aguilera *et al.*, "3D Printing of Electro Mechanical Systems," in *24th International SFF Symposium - An Additive Manufacturing Conference*, 2013.

[10] D. Espalin, D. W. Muse, E. MacDonald, and R. B. Wicker, "3D Printing multifunctionality: Structures with electronics," *The International Journal of Advanced Manufacturing Technology*, vol. 72, no. 5, pp. 963–978, 2014.

[11] MULTI3D, "100g Electrifi Conductive 3D Printing Filament." [Online]. Available: https://www.multi3dllc.com/product/electrifi-3d-printing-filament/.

[12] J. Mireles *et al.*, "Development of a Fused Deposition Modeling System for Low Melting Temperature Metal Alloys," *Journal of Electronic Packaging*, vol. 135, no. 1, p. 011008, 2013.

[13] P. Laakso, S. Ruotsalainen, E. Halonen, M. Mäntysalo, and A. Kemppainen, "Sintering of printed nanoparticle structures using laser treatment," in *Proceedings of 28th International Congress on Applications of Lasers & Electro-Optics*, 2009.

[14] K. Willis, E. Brockmeyer, S. Hudson, and I. Poupyrev, "Printed Optics: 3D Printing of Embedded Optical Elements for Interactive Devices," in *Proceedings of the 25th annual ACM symposium on User interface software and technology*, New York, 2012, p. 589.

[15] A. Kwas *et al.*, "Enabling Technologies for Entrepreneurial Opportunities in 3D printing of SmallSats," in *28 th Annual AIAA/USU Conference on Sma ll Sate llites*, 2014.

[16] F. Cuoghi, "The space additive revolution of CRP USA," *Reinforced Plastics*, vol. 60, no. 4, pp. 211–213, 2016.

[17] H. Zell, "NASA Boards the 3-D-Manufacturing Train," 2014. [Online]. Available: https://www.nasa.gov/content/goddard/nasa-boards-the-3-d-manufacturing-train/.

[18] E. MacDonald *et al.*, "3D Printing for the Rapid Prototyping of Structural Electronics," *IEEE Access*, vol. 2, pp. 234–242, 2014.

[19] M. Navarrete *et al.*, "Integrated Layered Manufacturing of a Novel Wireless Motion Sensor System with GPS," in *Solid Freeform Fabrication Symposium*, Austin, United States, 2007.

[20] C. Gutierrez *et al.*, "CubeSat Fabrication through Additive Manufacturing and Micro-Dispensing," *International Symposium on Microelectronics*, vol. 2011, no. 1, pp. 001021–001027, 2011.

[21] M. Vatani, Y. Lu, E. D. Engeberg, and J.-W. Choi, "Combined 3D printing technologies and material for fabrication of tactile sensors," *International Journal of Precision Engineering and Manufacturing*, vol. 16, no. 7, pp. 1375–1383, 2015.

[22] C. Shemelya *et al.*, "Encapsulated Copper Wire and Copper Mesh Capacitive Sensing for 3-D Printing Applications," *IEEE Sensors Journal*, vol. 15, no. 2, pp. 1280–1286, 2015.

[23] W. M. Marshall *et al.*, "Using Additive Manufacturing to Print a CubeSat Propulsion System," in *51st AIAA/SAE/ASEE Joint Propulsion Conference*, 2015.

[24] R. K. Masse, C. B. Carpenter, D. T. Schmuland, J. Overly, and M. Y. Allen, "CubeSat High-impulse Adaptable Modular Propulsion System (CHAMPS) Product Line Development Status and Mission Applications," in *49th AIAA/ASME/SAE/ASEE Joint Propulsion Conference*, Reston, Virginia, 2013.

[25] C. Shemelya *et al.*, "Anisotropy of thermal conductivity in 3D printed polymer matrix composites for space based cube satellites," *Additive Manufacturing*, vol. 16, pp. 186–196, 2017.

[26] R. M. Simon, "Emi Shielding Through Conductive Plastics," *Polymer-Plastics Technology and Engineering*, vol. 17, no. 1, pp. 1–10, 1981.

[27] Stratasys, "FDM Nylon 12CF DATA SHEET." [Online]. Available: http://www.stratasys.com/materials/search/fdm-nylon-12cf.

[28] EOS GmbH, "PA 2200 Product Information AHO / 03.10." [Online]. Available: https://www.sculpteo.com/static/0.30.0-49/documents/materials/polyamide_PA2200/PA2200_Product_information_03-10_en.pdf.

[29] "ULTEM 9085 PRODUCTION-GRADE THERMOPLASTIC FOR FORTUS 3D PRINTERS." [Online]. Available: http://www.stratasys.com/materials/search/ultem9085.

[30] EOS GmbH – Electro Optical Systems, "EOS PEEK HP3 Material Data Sheet," 2008. [Online]. Available: https://eos.materialdatacenter.com/eo/material/pdf/313792/EOSPEEKHP3?sLg=de&rnd=1524668637110.

[31] "Flying Laptop | | Universität Stuttgart." [Online]. Available: http://www.kleinsatelliten.de/flying_laptop/. [Accessed: 26-Apr-2018].